Distillation-Accelerated Uncertainty Modeling for Multi-Objective RTA Interception

Gaoxiang Zhao* Department of Applied Mathematics Harbin Institute of Technology, Weihai Weihai, China gaoxiang.zhao@stu.hit.edu.cn

> Rongjin Wang JD.COM Beijing, China wangrongjin3@jd.com

Ruina Qiu JD.COM Beijing, China qiuruinan1@jd.com

Zhangang Lin JD.COM Beijing, China linzhangang@jd.com

Pengpeng Zhao[†] JD.COM Beijing, China zhaopengpeng10@jd.com

Xiaoqiang Wang School of Mathematics and Statistics Shandong University Weihai, China xiaoqiang.wang@sdu.edu.cn

Abstract—Real-Time Auction (RTA) Interception aims to filter out invalid or irrelevant traffic to enhance the integrity and reliability of downstream data. However, two key challenges remain: (i) the need for accurate estimation of traffic quality together with sufficiently high confidence in the model's predictions-typically addressed through uncertainty modeling-and (ii) the efficiency bottlenecks that such uncertainty modeling introduces in real-time applications due to repeated inference. To address these challenges, we propose DAUM, a joint modeling framework that integrates multi-objective learning with uncertainty modeling, yielding both traffic quality predictions and reliable confidence estimates. Building on DAUM, we further apply knowledge distillation to reduce the computational overhead of uncertainty modeling, while largely preserving predictive accuracy and retaining the benefits of uncertainty estimation. Experiments on the JD advertisement dataset demonstrate that DAUM consistently improves predictive performance, with the distilled model delivering a tenfold increase in inference speed. Index Terms—Multi-objective Learning, Uncertainty Model-

ing, Distillation Acceleration

I. INTRODUCTION

In online advertising, RTA mechanisms play a central role in determining which traffic are exposed to downstream systems. Since not all incoming traffic contributes equally to campaign performance, an effective interception process is needed to filter out unproductive requests while preserving those that align with predefined objectives. Achieving this goal is particularly challenging because it requires not only the accurate prediction of multiple user-behavior metrics but also dependable estimates of prediction confidence under highly dynamic conditions. A natural way to address these requirements is to combine multi-objective optimization with uncertainty modeling. Multi-objective optimization methods, including PLE [1], MMOE [2], and ESMM [3], enhance performance by enabling knowledge sharing across related tasks such as Click-Through Rate (CTR) and Conversion Rate (CVR) prediction. Meanwhile, uncertainty modeling techniques—such as Bayesian Neural Networks (BNN) [4], Monte Carlo Dropout [5], and SWAG [6]—quantify prediction confidence by treating network weights as distributions and estimating variance through repeated inference. By integrating these components, RTA interception can rank incoming requests by their predicted contribution to downstream objectives, while at the same time adjusting uncertainty to reduce the risk of misinterpreting valuable traffic. In doing so, the framework improves both the effectiveness and the reliability of traffic selection.

In the context of RTA interception—particularly in our specific scenario-multi-objective modeling is leveraged to provide more accurate predictions by jointly optimizing multiple relevant objectives rather than focusing on a single one. At the same time, uncertainty modeling is incorporated to identify and pass traffic with high prediction uncertainty, thereby reducing the risk of mistakenly blocking valuable traffic. Together, these two components improve both the precision of prediction and the robustness of the interception process.

A major challenge in uncertainty modeling in RTA interception is handling extremely imbalanced labels [7], under which the prediction confidence may be inaccurate or misleading. Applying uncertainty modeling in such cases often leads to biased passing, which degrades overall model performance. A further challenge pertains to the computational efficiency of uncertainty modeling in RTA interception, as repeated inference can become a bottleneck in real-time scenarios. Methods such as BNN and SWAG can capture uncertainty effectively and improve overall performance; however, they require multiple forward passes during inference, imposing a significant computational overhead for real-time prediction. Models like EDL [8] can directly estimate uncertainty and achieve faster inference, but their predictive performance is generally inferior.

To address the challenge of ineffective traffic passing under highly imbalanced labels, we leverage uncertainty derived from relatively balanced metrics to guide the passing of traffic

^{*}Work done while interning at JD.COM

[†]Corresponding author

associated with imbalanced metrics. Through the integration of multi-objective optimization and uncertainty modeling, uncertainty estimates can be flexibly shared across different objectives, allowing the framework to adaptively manage both balanced and imbalanced metrics. This strategy enhances the selection of valuable traffic and increases the efficiency and robustness of downstream traffic passing.

To address the challenge of repeated inferences required by uncertainty modeling, we further introduce a distilled model that jointly predicts the original target labels and the variance outputs of the teacher uncertainty model, effectively transferring both predictive accuracy and uncertainty estimation. Our findings indicate that the output of the distilled model can be effectively utilized for passing high-uncertainty traffic, without the need for repeated inferences, thus improving efficiency.

The main contributions are summarized as follows:

- The internal mechanism of uncertainty modeling is analyzed, revealing that the uncertainty predicted for each sample is shaped by both the sample's properties and the conditional probabilities of its neighboring samples.
- A unified framework combining multi-objective optimization with uncertainty modeling is proposed, capable of estimating uncertainty under both balanced and imbalanced labels.
- A distilled uncertainty model is introduced, derived from the original model, which retains traffic passing capability while achieving 10x faster inference speed.

II. RELATED WORKS

Related works can be broadly grouped into three categories: (i) uncertainty modeling, (ii) multi-objective prediction, and (iii) approaches that integrate both uncertainty and multi-objective learning to simultaneously improve predictive performance and estimate model confidence.

A. Uncertainty modeling

Uncertainty modeling quantifies a model's uncertainty with respect to its inputs. Traditional approaches, which rely solely on the probabilities produced by cross-entropy outputs, often exhibit overconfidence, leading to incorrect traffic interception. In contrast, uncertainty modeling provides a more reliable estimate of prediction uncertainty, thereby enhancing the model's generalization capability.

Some approaches in uncertainty modeling enable the model to directly predict output uncertainty by assuming that the outputs follow a Gaussian distribution. A dedicated loss function is then employed to learn both the mean and the variance, with the variance serving as the measure of uncertainty:

$$y \sim \mathcal{N}(\mu(x), \sigma^2(x))$$
 (1)

Here, $\mu(x)$ denotes the model's predicted mean, and $\sigma^2(x)$ denotes the predicted variance. A loss function is designed to train both the mean and variance simultaneously:

$$\mathcal{L}(x,y) = \frac{1}{2}\log\sigma^{2}(x) + \frac{(y-\mu(x))^{2}}{2\sigma^{2}(x)}$$
(2)

This method exhibits high efficiency in both training and inference for uncertainty modeling and can effectively capture data uncertainty during training. However, its overall performance is suboptimal, primarily due to the strong assumptions imposed on the output distribution. Methods such as EDL replace direct class probabilities with dirichlet distribution parameters, which enables natural uncertainty quantification and alleviates the overconfidence issue commonly observed in traditional approaches, yielding better robustness on boundary and noisy samples. However, the overall predictive performance shows only limited improvement.

In addition, another class of uncertainty modeling methods represents each neuron in the network as a probabilistic distribution. These approaches perform multiple forward passes by sampling from the weight distribution, generating a set of outputs for a given input, with the variance across these outputs serving as a measure of the model's uncertainty for the input. For instance, in BNN, a probability distribution is assigned to each weight w:

$$w \sim q_{\theta}(w) \tag{3}$$

Here, $q_{\theta}(w)$ denotes variational approximation over the model weights. BNNs infer the posterior through variational inference:

$$p(w \mid D) \propto p(D \mid w)p(w) \tag{4}$$

By minimizing the KL divergence, the optimization objective is obtained by:

$$\mathcal{L} = \mathbb{E}_{q_{\theta}(w)}[\log p(D \mid w)] - \text{KL}(q_{\theta}(w) \parallel p(w))$$
 (5)

Afterwards, the model samples the weights multiple times to generate diverse outputs, and the variance across the outputs is used to measure uncertainty. However, BNNs are computationally expensive to train, and several lightweight methods have been proposed as approximations. For example, MC Dropout randomly drops neurons during inference, which is equivalent to sampling from an implicit weight distribution to estimate parameter uncertainty. Methods like SWAG collect weight trajectories during training and construct a distribution over the weights based on these trajectories:

$$p(\theta) = \mathcal{N}(\hat{\theta}, \Sigma) \tag{6}$$

Here, $p(\theta)$ represents the mean of the weights, and Σ denotes the covariance matrix constructed from the collected weights. With the weight distribution, multiple forward passes can be performed by repeatedly sampling. Compared with direct variance prediction methods, these weight-probabilistic approaches generally provide more reliable uncertainty estimation. However, repeated sampling during inference increases computational cost, which constrains real-time application.

B. Multi-Objective modeling

Multi-Objective learning in recommendation and advertising has evolved through several stages, progressing from simple dependency modeling to expert-based architectures and, more recently, to dynamic frameworks. Early work such

as ESMM addressed the sparsity challenge in CVR prediction by leveraging its dependency on CTR. By decomposing CVR into CTR and post-click conversion, ESMM enabled training over the entire sample space, thereby alleviating selection bias and significantly improving the accuracy of CVR estimation.

Building on this foundation, expert-based models sought to more effectively manage task heterogeneity. MMoE introduced a mixture-of-experts framework, where multiple experts are shared but task-specific gating networks determine expert selection, thereby reducing negative transfer and allowing greater flexibility in task representation. PLE extended this idea with a progressive layered extraction mechanism that disentangles shared and task-specific experts, providing a more structured balance between commonality and independence across tasks and mitigating the interference caused by conflicting objectives.

Subsequent work further emphasized explicit task dependency modeling. For example, AITM [9] adaptively transfers knowledge from upstream tasks such as CTR to downstream tasks such as CVR, thereby improving the learning of sparse objectives through direct exploitation of task relationships. Building on this idea, more recent approaches have focused on dynamic and scalable multi-task architectures. SNR [10] augments the shared-bottom paradigm with a neural router that dynamically allocates representations across tasks, while GRec [11] expands the expert framework with larger expert pools and sparse gating to enhance scalability in large-scale systems. Beyond structural improvements, methods such as MetaBalance [12] adopt meta-learning strategies to dynamically adjust task weights across objectives, improving adaptability under distribution shifts. AutoMTL [13] integrates neural architecture search, transfer learning, and dynamic routing into a unified framework, systematically decomposing multi-task learning into modular components.

Further advancing sparsity and control in expert routing, DSelect-k [14] introduces a continuously differentiable gate that selects at most k experts, enabling precise and efficient sparse activation in MoE-based recommenders. Meanwhile, industrial deployments have embraced hierarchical modeling: HiNet [15], employs a two-level interaction network to decouple shared user intent from scenario-specific behaviors, achieving strong generalization across heterogeneous traffic sources.

Collectively, these developments illustrate a clear trajectory toward more precise, flexible, and scalable modeling of task and scenario relationships, yielding substantial performance gains in modern recommendation and advertising systems.

C. Joint modeling of multi-objective learning and uncertainty quantification

While traditional multi-task learning focuses on optimizing multiple objectives simultaneously, recent advances recognize that explicitly quantifying prediction uncertainty is crucial for robust decision-making in recommendation and advertising systems. This has spurred the development of frameworks that jointly model task relationships and uncertainty, progressing

from simple loss reweighting to principled Bayesian formulations and gradient-level uncertainty integration.

A foundational approach was proposed by Kendall et al. [16], introducing a method to weight each task's loss according to its task-dependent uncertainty. By treating uncertainty as a learnable parameter, this approach automatically balances the relative importance of tasks—assigning lower weight to noisier or sparser objectives such as conversion rate (CVR)—without requiring manual tuning. Due to its simplicity and effectiveness, this uncertainty-aware loss weighting has since become a standard technique in multi-objective recommendation systems.

This principle has been extended to semi-supervised and distillation-based settings, where label noise or sparsity is particularly severe. For example, UKD [17] combines uncertainty modeling with knowledge distillation to tackle the extreme sparsity of conversion labels. It employs a "click-adaptive" teacher model to generate reliable pseudo-conversion-rate labels for unclicked advertisements, and the student model is subsequently trained on both observed clicked conversions and these pseudo labels. Importantly, the student quantifies its prediction uncertainty via the discrepancy between its internal dual predictors, assigning lower loss weights to samples with higher uncertainty. This mechanism effectively mitigates the impact of noisy pseudo labels and corrects prediction bias for non-clicked ads, illustrating how uncertainty-aware weighting can be extended beyond multi-task loss settings to distillation and label completion scenarios.

More recently, uncertainty has been leveraged at the optimization level to resolve gradient conflicts among competing objectives. Achituve et al. [18] introduced a Bayesian gradient aggregation method that treats task-specific gradients as random variables and fuses them according to their uncertainty. This approach stabilizes training and improves generalization, especially when tasks exhibit strong interference or distributional shifts.

In interactive and personalized settings, uncertainty is also integrated into the objective space itself. Wang et al. [19] proposed an orthogonal meta-learning enhanced Bayesian optimization framework that captures user-specific trade-offs between objectives while accounting for uncertainty in preference estimation. By constructing personalized Pareto fronts under uncertainty, this method enables more ethical and adaptive multi-stakeholder recommendations.

Collectively, these studies indicate that uncertainty modeling has become an essential component of multi-objective prediction. By jointly estimating target outcomes and their associated confidence, these approaches improve prediction accuracy, support more reliable decision-making, and enhance adaptability in dynamic recommendation and advertising environments.

III. MAIN WORKS

In this section, we first present a mathematical formulation of the interception scenario and outline the motivation for incorporating uncertainty modeling. We then quantify uncertainty in the context of real-time advertising auctions, highlighting its advantages over conventional probability predictions based on cross-entropy, and analyze the scenarios in which uncertainty modeling is effective and fails. Following this, we introduce the integration of multi-objective modeling and uncertainty to address the limitations of uncertainty modeling in imbalanced data scenarios, and subsequently present the overall structure of the proposed DAUM. Finally, we present the design principles behind the distillation framework, which effectively enhances model inference efficiency while preserving robust uncertainty measurement capabilities.

A. Interception scenario formalization

The interception scenario aims to maximize the quality of downstream traffic while limiting the interception rate. In this context, the optimization goal is to selectively block low-quality traffic to enhance overall traffic quality:

obj.
$$\max \sum_{i} e_{i} \cdot z_{i}$$
s.t.
$$\frac{\sum_{i} (1 - z_{i})}{N} = r$$

$$z_{i} \in \{0, 1\}, \quad \forall i$$

$$(7)$$

Let $z_i \in \{0,1\}$ denote the intercept/pass decision, with $z_i = 1$ indicating a pass, r represents our interception ratio, which dynamically changes with consumption. Due to the sufficient traffic, we select the best (1-r) fraction of traffic to pass downstream in order to enhance conversion efficiency. e_i represents the expected reward of the i-th sample, which, in our scenario, is jointly evaluated based on four metrics—has C2S click, online, add to cart, and deal:

$$e_i = f(t_1, t_2, t_3, t_4)$$
 (8)

C2S refers to whether a user performs an advertisement click in the context of all advertisements displayed on external platforms. Online denotes whether, among users who have clicked on an advertisement, they subsequently land on the JD website. Add to Cart and Deal describe the actions of users who have landed on the JD website, specifically whether they add products to their shopping cart or complete a transaction, respectively. These metrics follow a hierarchical structure and are interrelated. The function f can be configured in different forms according to business requirements. For instance, if we want to emphasize the deal metric, we formulate a function fthat adjusts the influence of this metric during optimization, enabling the model to better align with specific business objectives. t_i represents the score corresponding to each metric. This score is determined by both the model's predicted score and the uncertainty of the prediction:

$$t_i = h(s_i, u_i) \tag{9}$$

where s_i represents the mean of the model's output for the i_{th} metric, and u_i denotes the corresponding uncertainty. h represents our strategy for combining uncertainty and predicted scores. In the interception scenario, h should exhibit a positive relationship with both uncertainty and predicted scores in order

to prevent the misclassification or exclusion of valuable traffic. In our specific setting, the most uncertain instances are directly classified as positive, while the remaining instances are classified based on their predicted scores. The design of h is not fixed and can be adjusted according to the requirements of the specific scenario. To achieve better predictions and flexibly adapt to various scenarios, we introduce multi-objective modeling to handle each metric while also providing its associated uncertainty. We target confident interception of low-quality traffic, defined as instances with low predicted probabilities and high prediction confidence. Traditional probability outputs often suffer from overconfidence, leading to the interception of potentially valuable traffic. To address this issue, we introduce uncertainty modeling, which we mathematically demonstrates that this uncertainty measure, by considering the uncertainty of neighboring samples, helps mitigate the overconfidence problem.

B. Intrinsic logic of uncertainty modeling

The instances with high uncertainty represent cases where the model's predictions lack confidence. The objective is to pass truly high-uncertainty samples—i.e., samples where the model's classification capability is insufficient—so as to avoid incorrectly intercepting valuable traffic and improve the overall quality of the downstream traffic. Confidence based on cross-entropy output probabilities often suffers from overconfidence, whereas explicit uncertainty modeling mitigates this issue by considering the context of surrounding samples. We begin by outlining how uncertainty modeling quantifies uncertainty in our scenario and its uniqueness compared to cross-entropy output.

We first define the uncertainty in our scenarios, focusing on ambiguous users, i.e., those who share the same feature vector x^* but have different labels y_1, y_2, \ldots, y_m . Formally, the conditional probability is defined as:

$$q = P(y = 1 \mid x^*) = \frac{1}{m} \sum_{i=1}^{m} y_i, \quad 0 < q < 1$$
 (10)

For ambiguous users, the conditional probability lies strictly between 0 and 1.

The update rule of SGD is given by:

$$w^{(t+1)} = w^{(t)} - \eta \cdot \nabla_w \ell(w^{(t)}; x^*, y) \tag{11}$$

The change in the model prediction is:

$$\begin{split} f_{w^{(t+1)}}(x^*) &= f_{w^{(t)}}(x^*) + \nabla_w f_{w^{(t)}}(x^*)^\top \left(w^{(t+1)} - w^{(t)} \right) \\ &+ o\left(\| w^{(t+1)} - w^{(t)} \| \right) \end{split}$$

By neglecting higher-order terms, we approximate:

$$f_{w^{(t+1)}}(x^*) \approx f_{w^{(t)}}(x^*) + \nabla_w f_{w^{(t)}}(x^*)^\top \left(w^{(t+1)} - w^{(t)}\right)$$

Substituting the SGD update 11 gives:

$$f_{w^{(t+1)}}(x^*) \approx f_{w^{(t)}}(x^*) - \eta \cdot \nabla_w f_{w^{(t)}}(x^*)^\top \nabla_w \ell(w^{(t)}; x^*, y)$$
(12)

Let $\ell(w; x^*, y)$ be the loss function, $\sigma(\cdot)$ the sigmoid function, and $f_w(x^*)$ the model output. The gradient of the loss with respect to the weights is:

$$\nabla_w \ell(w; x^*, y) = (\sigma(f_w(x^*)) - y) \cdot \nabla_w f_w(x^*)$$

Let $c = \|\nabla_w f_w(x^*)\|^2 > 0$, using gradient descent with learning rate η , the updated model output 12 is approximated as:

$$f_{w^{(t+1)}}(x^*) \approx f_{w^{(t)}}(x^*) - \eta c(\sigma(f_w(x^*)) - y)$$
 (13)

We define the ideal prediction value f^* such that its activation probability satisfies the condition probability at the contradiction point:

$$\sigma(f^*) = q.$$

We define the error term as:

$$e_t = f_{w^{(t)}}(x^*) - f^* (14)$$

which represents the difference between the current prediction and the optimal prediction. When SGD approaches convergence, we can linearize $\sigma(f_w(x^*))$, at f^* , we get:

$$\sigma'(f^*) = \sigma(f^*)(1 - \sigma(f^*)) = q(1 - q)$$

Therefore, we can perform a linear approximation of the prediction:

$$\sigma(f_w(x^*)) \approx \sigma(f^*) + \sigma'(f^*) \cdot (f_w(x^*) - f^*) = q + q(1 - q)e_t$$
(15)

Substituting 15 into the update formula of the predictiton 13, we have:

$$f_{w^{(t+1)}}(x^*) \approx f_{w^{(t)}}(x^*) - \eta c \left(\sigma(f_{w^{(t)}}(x^*)) - y\right)$$

= $f^* + \left[1 - \eta c q(1-q)\right] e_t + \eta c(y-q)$

Thus, the update rule of the error term can be derived as:

$$e_{t+1} = f_{w^{(t+1)}}(x^*) - f^*$$

$$\approx \left[1 - \eta c q (1-q)\right] e_t + \eta c (y-q)$$
(16)

The update process in 16 follows an AR(1) random process

$$e_{t+1} = \alpha e_t + \epsilon_t,$$

where $\alpha = 1 - \eta cq(1-q)$ and $\epsilon_t = \eta c(y-q)$. When $\alpha < 1$, the stationary variance of this process is

$$Var(e_t) = \frac{Var(\epsilon_t)}{1 - \alpha^2}.$$
 (17)

We compute separately:

$$Var(\epsilon_t) = Var(\eta c(y - q))$$

$$= (\eta c)^2 Var(y)$$

$$= (\eta c)^2 q(1 - q).$$
(18)

And:

$$1 - \alpha^2 = 1 - \left[1 - \eta cq(1 - q)\right]^2$$

= $\eta cq(1 - q)\left[2 - \eta cq(1 - q)\right].$ (19)

Thus.

$$Var(e_t) = \frac{(\eta c)^2 q (1 - q)}{\eta c q (1 - q) [2 - \eta c q (1 - q)]}$$
$$= \frac{\eta c q (1 - q)}{2 - \eta c q (1 - q)}.$$
 (20)

This is the uncertainty measure derived from the weighted probability-based approach. We now analyze the properties of this formulation. The closer q is to 0.5, the higher the uncertainty; conversely, the farther q deviates from 0.5, the lower the uncertainty. The coefficient c denotes the gradient of the sample with respect to the weight at this point. Intuitively, when a sample's uncertainty deviates from that of its neighboring samples, the overall uncertainty increases.

We next present a mathematical analysis of how neighboring samples affect the uncertainty of a given sample. We illustrate this problem using a simple binary classification task, assume the output layer of the binary classifier is:

$$q(x; w) = \sigma(w^{\top} \phi(x))$$

The gradient of the output with respect to the weights at x_1 can be written as:

$$g_1 := \nabla_w q(x_1; w) = s_1 \phi_1, \quad s_1 := q_1(1 - q_1), \quad \phi_1 := \phi(x_1).$$

Its Hessian matrix is:

$$H_1 := \nabla_w^2 q(x_1; w) = q_1 (1 - q_1) (1 - 2q_1) \phi_1 \phi_1^{\top}$$

= $s_1 (1 - 2q_1) \phi_1 \phi_1^{\top}$. (21)

Suppose we already have x_1 , and then train on x_2 . We assume a common phenomenon in industrial scenarios, where similar users may exhibit inconsistent behaviors. Specifically, if x_1 and x_2 are sufficiently close, but the true conditional probability of x_2 is inconsistent with that of x_1 . The crossentropy loss in this case is:

$$BCE(y, q(x_2; w)) = -y \cdot \log(q(x_2; w)) - (1 - y) \cdot \log(1 - q(x_2; w))$$

 $q(x_2; w)$ represents the probability output for x_2 before updating weights. We compute the average gradient over all x_2 , yielding:

$$-[q_2 \cdot \log(q(x_2; w)) + (1 - q_2) \cdot \log(1 - q(x_2; w))]$$

The gradient of this loss is:

$$\nabla_w \ell = (q(x_2; w) - q_2) \cdot \nabla_w q(x_2; w) = (q_2^{\text{pred}} - q_2) \cdot s_2 \phi_2$$

Thus, the parameter update is:

$$\Delta w = -\eta \nabla_w \ell = -\eta (q_2^{\text{pred}} - q_2) s_2 \phi_2 \tag{22}$$

Since x_1 and x_2 are close enough and f is smooth, before training x_2 , the model's prediction for x_2 should be close to that of x_1 , which is:

$$q_2^{\mathrm{pred}} pprox q_1^{\mathrm{pred}} pprox q_1$$

After substitution in 22, the gradient update becomes:

$$\Delta w \approx -\eta (q_1 - q_2) s_2 \phi_2$$

Thus, the effect on the gradient is:

$$\Delta g_1 \approx H_1 \Delta w = s_1 (1 - 2q_1) \phi_1 \phi_1^{\top} \left[-\eta (q_1 - q_2) s_2 \phi_2 \right]$$

= $-\eta s_1 s_2 (1 - 2q_1) (q_1 - q_2) (\phi_1^{\top} \phi_2) \phi_1$ (23)

We compute the relative change in norm:

$$\frac{\Delta \|g_1\|}{\|g_1\|} \approx -\eta s_2 (1 - 2q_1) (q_1 - q_2) \frac{\phi_1^\top \phi_2}{\|\phi_1\|} \cdot \frac{s_1}{\|g_1\|}$$
 (24)

Thus, the change of c is determined by:

$$(1-2q_1)(q_2-q_1)\phi_1^{\mathsf{T}}\phi_2$$
 (25)

The larger the inner product between features—indicating higher similarity between two samples—the greater its influence on c. Moreover, the magnitude and direction of the change in c also depend explicitly on the values of q_1 and q_2 . Specifically, if q_1 exhibits a tendency toward predicting the negative class (i.e., $q_1 < 0.5$), then the uncertainty increases when q_2 demonstrates a relatively stronger inclination toward the positive class compared to q_1 ; conversely, the uncertainty decreases when q_2 shows a relatively stronger inclination toward the negative class relative to q_1 .

C. Analysis of effective and ineffective uncertainty scenarios

By analyzing 20 and 25, the role of uncertainty modeling can be decomposed into two parts, for equation:

$$\frac{\eta cq(1-q)}{2-\eta cq(1-q)}.$$

The first part is the predicted probability, where uncertainty increases as the predicted probability approaches 0.5. The second part is the influence of neighboring samples on c, which can be regarded as a correction strategy:

$$(1-2q_1)(q_2-q_1)\phi_1^{\top}\phi_2$$

This can be interpreted as follows: for similar samples, despite the potential differences in label proportions, uncertainty modeling tends to provide consistent uncertainty measures. Given that the uncertainty of an individual point often exhibits significant fluctuations, incorporating neighboring points leads to a more stable uncertainty prediction, thereby enhancing the robustness of the model.

However, the conventional approach to uncertainty modeling suffers from significant limitations in the presence of class-imbalanced data. Notably, both the standard variance-based uncertainty measure q(1-q) and the correction term c implicitly adopt 0.5 as the reference point for quantifying uncertainty. This assumption is well-justified under class-balanced conditions: when the input features provide no discriminative information, a well-calibrated model tends to output a prediction score $q\approx 0.5$, reflecting maximal epistemic uncertainty (i.e., the model is equally uncertain about assigning the sample to either class). Formally, under balanced settings, the expected prediction for an uninformative instance is

$$\mathbb{E}[q \mid \text{uninformative features}] = 0.5,$$
 (26)

and the associated predictive variance q(1-q) attains its maximum at this point, correctly indicating high uncertainty.

In contrast, under severe class imbalance—particularly when the positive class is rare—the model's predictions are systematically biased toward lower probabilities. For uninformative samples, the model no longer predicts $q\approx 0.5$, but instead outputs a value close to the empirical base rate $\pi=\frac{N_+}{N}\ll 0.5$, where N_+ and N denote the numbers of positive and total samples, respectively. Consequently, the general prediction under imbalance is approximately $q\approx \pi$, not 0.5. Persisting in using 0.5 as the uncertainty reference introduces substantial bias, which is further supported by the results of our experiments. Specifically, a prediction of q=0.5 in such a context is, in fact, highly confident—indicating strong belief in the positive class—yet the standard uncertainty metric q(1-q) would misleadingly interpret it as maximally uncertain:

$$q(1-q)\big|_{q=0.5} = 0.25, (27)$$

despite the fact that, under imbalance, $q=0.5\gg\pi$ represents a significantly high prediction score. Nevertheless, conventional uncertainty modeling would erroneously classify such a sample as highly uncertain, thereby undermining the reliability of downstream decision-making based on uncertainty estimates. Similarly, the correction term c also becomes entirely ineffective under sparse metrics: when the indicator is sparse, $(1-2q_1)$ is always positive, and if q_2 exhibits a stronger tendency toward predicting the positive class than q_1 , the uncertainty paradoxically increases—a result that indicates complete failure of the correction mechanism.

D. DAUM

We have previously demonstrated the failure of uncertainty modeling on imbalanced metrics. Currently, there is no effective solution through weight-based probabilistic methods. However, in the multi-objective prediction framework, different metrics are not independent but exhibit certain correlations. Given that uncertainty modeling works well on balanced metrics and that the metrics are correlated, we can replace the biased uncertainty produced on imbalanced metrics with the accurate uncertainty derived from balanced metrics. As the correlation between the two metrics strengthens, the shared uncertainty effect can become more effective, and thus the model's overall uncertainty modeling performance improves. In our scenario, positive samples for both add-to-cart and deal labels are sparse. When samples with high uncertainty in the add-to-cart or deal predictions are directly passed, inaccurate estimation of minority-class uncertainty may cause misclassification of instances that could otherwise be correctly classified, resulting in increased resource waste. We address this problem with the DAUM model, leveraging uncertainty information shared across multiple objectives to supplant inaccurate single-metric estimates, thereby enhancing the accuracy and confidence of traffic interception. We first present the overall framework of DAUM, a modeling approach that integrates multi-objective learning with uncertainty modeling. The complete framework is illustrated in Figure 1:

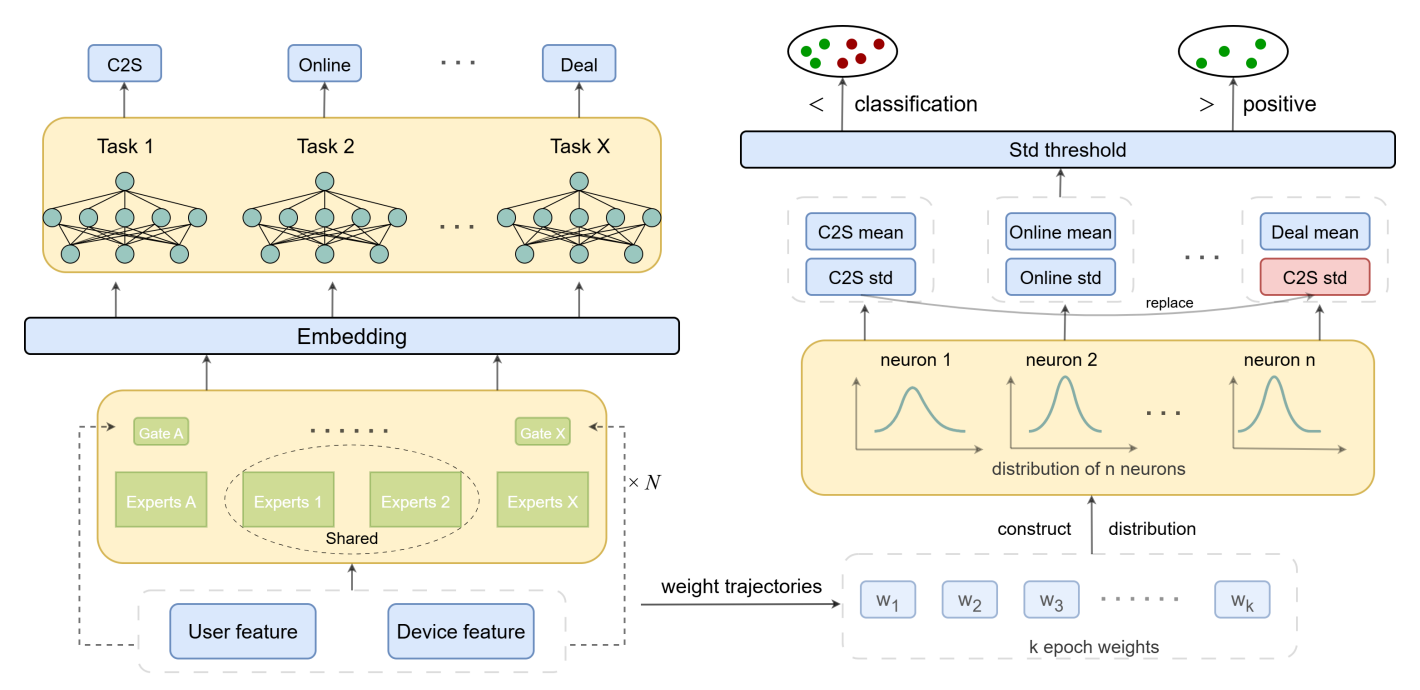


Fig. 1: The main network of DAUM model. We first train the model using the PLE structure and collect the model weights from the last k epochs. For each neuron, we construct a Gaussian distribution based on these k sets of weights. We then perform multiple samplings from the weight distributions to compute the mean and variance of the outputs for each target. Finally, according to interception requirements, we apply a threshold on the predicted uncertainty: samples with high uncertainty are directly passed, while low-uncertainty samples are processed through the standard classification procedure.

DAUM is a two-stage model designed to integrate multiobjective learning with uncertainty modeling for interception scenarios. In the first stage, a multi-objective model is trained across multiple targets to capture task-specific patterns and dependencies. The propagation of shared representations across tasks follows:

$$\mathbf{h}^{(t)} = f_{\theta}^{(t)} \left(\mathbf{h}^{(t-1)}, \mathbf{g}_{\text{shared}} \right), \quad t = 1, \dots, T$$
 (28)

where $\mathbf{h}^{(t)}$ is the task-specific hidden state for target t, $\mathbf{g}_{\mathrm{shared}}$ is the shared representation, and $f_{\theta}^{(t)}$ denotes the task-specific transformation.

In the second stage, uncertainty is estimated using the weight trajectories collected during training via SWAG. We sample weights \mathbf{w}_k from the approximate posterior as:

$$\mathbf{w}_k = \boldsymbol{\mu}_{\text{SWA}} + \frac{1}{\sqrt{2}} \mathbf{\Sigma}_{\text{diag}}^{1/2} \boldsymbol{\zeta}_1^{(k)} + \frac{1}{\sqrt{2(K-1)}} \mathbf{D} \boldsymbol{\zeta}_2^{(k)}$$
 (29)

where $\mu_{\rm SWA}$ is the stochastic weight average, $\Sigma_{\rm diag}$ is the diagonal covariance estimate, ${\bf D}$ contains the top K deviation vectors from the SWA trajectory, and ${\bf \zeta}_1^{(k)}, {\bf \zeta}_2^{(k)} \sim \mathcal{N}(0,{\bf I})$ are standard Gaussian noise vectors for the k-th sample. Multiple samples $(k=1,\ldots,K)$ are drawn to estimate predictive uncertainty.

DAUM allows uncertainty to be modeled across multiple targets simultaneously, note that in our scenario, the uncertainty of the deal label is replaced by the uncertainty of the C2S click label. This adjustment is made because the

uncertainty derived from sparse labels is typically inaccurately estimated. However, multi-objective modeling can effectively mitigate this issue by sharing uncertainty across objectives. This approach will be further validated in the experimental section that follows.

E. Distillation of DAUM

DAUM demonstrates strong performance in both prediction accuracy and interception capability. However, uncertainty modeling requires multiple inferences during prediction, which poses significant challenges for real-time online inference. To address this issue, we propose a dual-objective submodel for each target that jointly learns the true classification labels and the uncertainty outputs provided by DAUM.

It should be noted that the losses of distilled uncertainty labels and classification labels typically differ in magnitude. Joint training can cause the base model to be dominated by the classification loss, leaving insufficient signal for uncertainty learning. Since uncertainty-based interception is generally related to proportions rather than absolute values, we rescale the uncertainty labels so that their mean matches that of the classification labels. This enables the distilled model to effectively learn uncertainty while significantly improving online inference efficiency. The complete inference procedure is summarized in Algorithm 1.

IV. EXPERIMENTS

In this section, we present the main experimental results. We begin by describing the characteristics of the data collected Algorithm 1 Uncertainty-Aware Multi-Task Binary Classification

```
Require: User features x, training rounds K, final k_{\text{small}}
         rounds for SWAG, number of samples M, uncertainty
threshold 	au, number of objectives T
Ensure: Prediction vector \mathbf{y}_{\text{pred}} = [y_{\text{pred}}^{(1)}, \ldots, y_{\text{pred}}^{(T)}], where
   y_{\text{pred}}^{(t)} \in \{-1, +1\} 1: Train multi-task model (shared backbone + T task-specific
         heads) for K rounds
   2: Collect weights from final k_{\text{small}} rounds: W
  \{\theta_t\}_{t=K-k_{\rm small}+1}^K 3: Compute SWAG statistics for shared backbone:
              \bar{\theta} \leftarrow \frac{1}{k_{\text{small}}} \sum_{\theta \in \mathcal{W}} \theta
              Construct deviation matrix D \in \mathbb{R}^{d \times r} from last r
         weight differences
  6: \Sigma_{\mathrm{diag}} \leftarrow \mathrm{diag}\left(\frac{1}{k_{\mathrm{small}}}\sum_{\theta \in \mathcal{W}}(\theta - \bar{\theta})^2\right)
7: for each task t = 1 to T do
              Initialize prediction set: S_t \leftarrow \emptyset
  9: end for
 10: for sample m = 1 to M do
             Sample \mathbf{z}_1 \sim \mathcal{N}(0, I_r), \ \mathbf{z}_2 \sim \mathcal{N}(0, I_d)

\theta^{(m)} \leftarrow \bar{\theta} + \frac{1}{\sqrt{2}} D\mathbf{z}_1 + \frac{1}{\sqrt{2}} \Sigma_{\mathrm{diag}}^{1/2} \mathbf{z}_2

for each task t = 1 to T do
p_t^{(m)} \leftarrow f_t(\mathbf{x}; \theta^{(m)}) \text{ {Head } } t \text{ outputs probability for}
 11:
 12:
 13:
 14:
                   \mathcal{S}_t \leftarrow \mathcal{S}_t \cup \{p_t^{(m)}\}
 15:
              end for
 16:
 17: end for
 18: for t = 1 to T do
             \mu_t \leftarrow \frac{1}{M} \sum_{p \in \mathcal{S}_t} p, \quad \sigma_t^2 \leftarrow \frac{1}{M} \sum_{p \in \mathcal{S}_t} (p - \mu_t)^2
if \sigma_t^2 \geq \tau then
y_{\text{pred}}^{(t)} \leftarrow +1 \text{ {Conservative: predict positive if uncertain)}}
 19:
 20:
 21:
 22:
                  y_{\text{pred}}^{(t)} \leftarrow \begin{cases} +1 & \text{if } \mu_t > 0.5 \\ -1 & \text{otherwise} \end{cases}
 23:
 24:
 25: end for
26: return \mathbf{y}_{\text{pred}} = [y_{\text{pred}}^{(1)}, \dots, y_{\text{pred}}^{(T)}]
```

from the advertising scenario. We then compare the classification performance of several models across multiple objectives. The results indicate that DAUM consistently outperforms competing methods, achieving both stronger classification capability and enhanced interception effectiveness.

Next, we highlight the challenge of interception failure under severe class imbalance. We show DAUM enables a more accurate estimation of uncertainty for minority classes. Finally, we evaluate the distilled model in terms of accuracy and uncertainty estimation performance. Compared to the original uncertainty model, the distilled model maintains similar predictive accuracy while significantly reducing inference time, making it suitable for real-time inference scenarios.

A. Datasets

We first introduce the dataset used for training and evaluation, collected from the JD advertising system. Each traffic instance contains 108 features covering user and device-level attributes. We randomly sample 1 million instances, with 80% used for training and 20% for testing.

Our previous analysis shows that uncertainty modeling is highly correlated with the proportion of positive samples. To this end, we briefly describe the sparsity of positive samples in our data. Among the four metrics, C2S click is the most balanced, while online is relatively more imbalanced in comparison to C2S click. Both add to cart and deal are extremely sparse metrics, with deal being the sparsest.

B. Effect of multi-objective learning

In this section, we first verify that multi-objective and uncertainty modeling can improve prediction accuracy in our advertising scenario. We compare five models: MLP, PLE with MLP as the base expert, Transformer, PLE with Transformer as the base expert, and DAUM built upon PLE-Transformer, where the predicted values are obtained by averaging multiple predictions drawn from the uncertainty model. All multi-task models are implemented with three shared experts and one task-specific expert per task. The four objectives are C2S click, online, add to cart, and deal. The comparative results are summarized in Table I:

PLE-Transformer achieved the second-best overall performance, suggesting that integrating multi-objective learning with the Transformer architecture enables the capture of more complex patterns. Building on this, DAUM leverages the mean output from uncertainty modeling and outperforms in 7 out of 8 metrics. These results indicate that uncertainty modeling provides additional information for multi-objective tasks, thereby enhancing predictive performance.

C. Evaluation of passing capability

In the interception scenario designed for DAUM, we investigate whether uncertainty modeling, by passing samples with high uncertainty that the model cannot reliably classify, improves classification performance on the residual traffic. In our experiments, C2S click and deal traffic are passed using C2S click-based and deal-based uncertainty, respectively. We further evaluate the model's performance on deal traffic passed by C2S click-based uncertainty. For the deal task, the passing ratio is accordingly lowered due to the sparsity of positive samples. The model's performance on the residual traffic is summarized in Table II.

We observe that for the C2S click task, where positive and negative samples are relatively balanced, passing high-uncertainty traffic improves classification performance on the residual traffic. In contrast, in scenarios with sparse positive samples, passing high-uncertainty traffic can degrade model performance. The underlying logic of uncertainty modeling become ineffective is that it relies on a 0.5 decision boundary. However, this assumption fails when the overall prediction distribution is shifted, leading to biased uncertainty estimation.

TABLE I: Performance comparison of different models on four tasks.

Target	MLP		Transformer		PLE-MLP		PLE-Transformer		DAUM	
	AUC-ROC	AUC-PR	AUC-ROC	AUC-PR	AUC-ROC	AUC-PR	AUC-ROC	AUC-PR	AUC-ROC	AUC-PR
C2S click online add to cart deal	0.8084 0.7171 0.7865 0.7797	0.8629 0.7616 0.2568 0.1113	0.8094 0.7188 0.7934 0.7895	0.8640 0.7640 0.2605 0.1173	0.8078 0.7163 0.7909 0.7904	0.8624 0.7615 0.2581 0.1152	0.8094 0.7203 0.7947 0.7959	0.8639 0.7651 0.2622 0.1211	0.8097 0.7218 0.7965 0.7962	0.8642 0.7667 0.2646 0.1191
Average	0.7729	0.4982	0.7778	0.5015	0.7764	0.4993	0.7801	0.5031	0.7811	0.5037

TABLE II: Model performance under different passing ratios

C2S cl	ick traffic pass	ing	Deal	l traffic passing	g	C2S click-based passing on deal traffic			
Passing ratio	AUC-ROC	AUC-PR	Passing ratio	AUC-ROC	AUC-PR	Passing ratio	AUC-ROC	AUC-PR	
0.20 0.15 0.10 0.05 0	0.8290 0.8245 0.8196 0.8146 0.8097	0.8880 0.8820 0.8760 0.8701 0.8642	0.020 0.015 0.010 0.005 0	0.7890 0.7911 0.7926 0.7944 0.7962	0.1053 0.1088 0.1112 0.1154 0.1191	0.020 0.015 0.010 0.005 0	0.7972 0.7970 0.7966 0.7968 0.7962	0.1178 0.1186 0.1182 0.1192 0.1191	

We note that uncertainty is accurately modeled for the C2S click metric. When focusing on the deal metric, we can leverage uncertainty sharing to pass deal traffic based on C2S click uncertainty, thereby improving overall pass performance on the deal metric.

It is noteworthy that AUC-PR is a metric that is significantly influenced by the proportion of positive samples. In sparse metrics, as the passing ratio increases, a decline in AUC-PR is a reasonable trend, and attention should be focused on the relative changes between the two passing strategies.

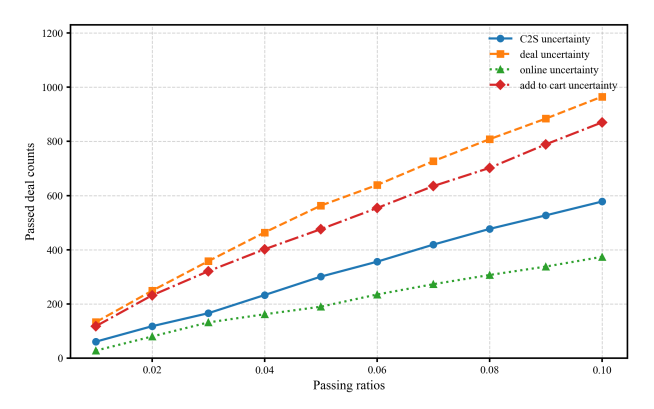
Next, we proceed to evaluate the performance of indirect passing from multiple perspectives. Specifically, we design three experiments on the deal dimension by varying the ratio of direct passing. These experiments examine: (i) the number of deal samples passed under the uncertainty threshold, (ii) the number of deal samples that can be classified among the remaining traffic, and (iii) the total number of deal samples by summing both the directly passed deal traffic and the remaining deal traffic that can be correctly classified, which aligns with industry scenarios, where we assess how many deal orders are passed downstream. These experiments evaluate how uncertainty influences deal prediction across different passing strategies. To further address potential reliability issues arising from inconsistent outcomes under different passing strategies, we conduct an additional experiment in which the number of directly passed deal samples is fixed, and we observe the proportion of deal samples that can still be correctly classified among the remaining traffic. The results are summarized in Figure 2.

Figures 2a and 2b primarily analyze the preferences of various passing strategies. It can be observed that, for uncertainty models derived from sparse metrics such as add to cart and deal, the model is more likely to directly pass deal samples, whereas more balanced metrics show a relative preference for passing mixed samples. Accordingly, for the remaining traffic,

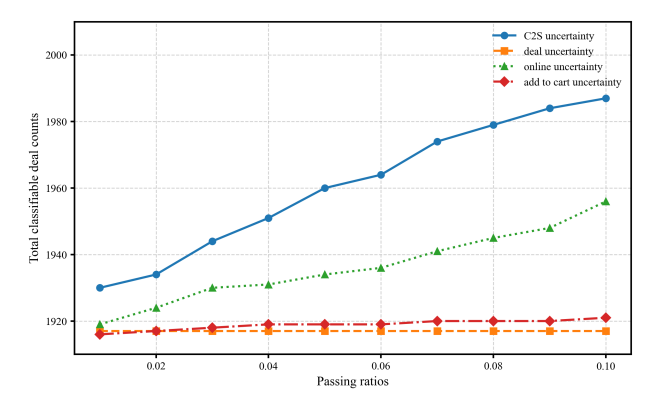
strategies that pass more deal samples directly tend to quickly reduce the number of identifiable deal samples, which is an expected outcome.

To further illustrate the results, we observe the total number of deal samples passed downstream, which includes both the number of positive samples directly passed and the number of positive samples that can be classified from the remaining traffic, as shown in Figure 2c. As the passing ratio increases, both balanced metrics like C2S click and online effectively pass more deal samples downstream. However, for imbalanced metrics, the total number of deal samples passed to downstream remains nearly unchanged. This phenomenon aligns with the previously analyzed conclusion that uncertainty modeling fails on imbalanced samples. To be more specific, uncertainty for sparse metrics results in high-probability samples being classified as high-uncertainty, despite these high-probability samples already being correctly classified, this indicates that passing based on imbalanced uncertainty is entirely ineffective, which also explains why the number of deal-completing samples passed downstream remains almost unchanged as the passing ratio increases. In contrast, uncertainty derived from balanced metrics is not affected by imbalance and, due to the correlation between metrics, provides effective information for uncertainty modeling on imbalanced metrics.

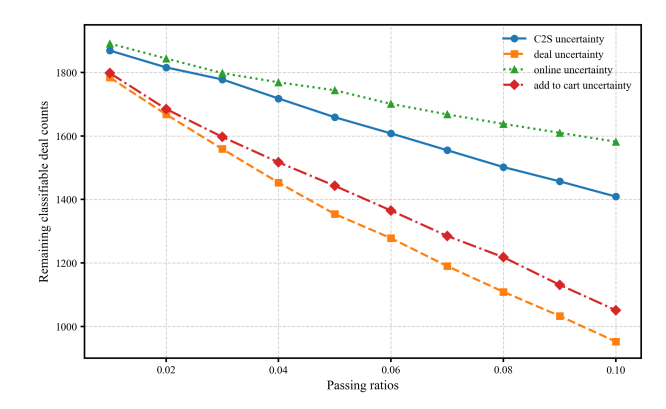
Different uncertainties exhibit varying passing preferences for deal samples, and these passing tendencies may lead to unfair comparisons. For example, a strategy that favors passing deal samples may yield greater benefits for the model at first; however, its performance may degrade as the passing ratios increase. In contrast, a strategy that favors passing negative samples may initially perform poorly, but later, as the passing ratios increase, there may be a rapid increase in the total number of deal samples passed. To further demonstrate the capabilities of the indirect passing strategy, we control for different passing ratios and ensure that all strategies directly



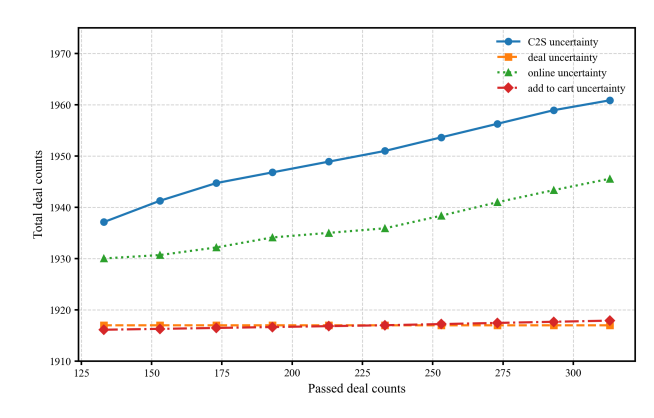
(a) The number of deal samples in directly passed samples with respect to passing samples.



(c) The number of deal samples with respect to passing samples.



(b) The number of deal samples in remaining samples with respect to passing samples.



(d) The number of deal samples with respect to passed deal samples.

Fig. 2: The number of valid deal samples passed to downstream with respect to passing ratio and the number of deal samples passed.

pass the same number of deal samples, as shown in Figure 2d, we find that the effect of indirect passing is significantly better on balanced metrics compared to imbalanced metrics. Indirect passing relies on the correlation between metrics and the balance of metrics. If more relevant and balanced metrics are used, the number of deal samples passed downstream is likely to increase.

D. Model distillation

Uncertainty modeling requires multiple inferences during prediction, which poses challenges for real-time applications. To address these efficiency concerns while retaining the benefits of uncertainty modeling in interception scenarios, we propose a distillation method that treats the uncertainty predicted by the original model as a secondary objective. An additional output layer is added to the student model to simultaneously generate both predictions and uncertainty estimates. The passing ability of the distilled model on the C2S click task is summarized in Figure 3:

Distilled uncertainty significantly improves the classification capability on the residual traffic by passing high-uncertainty samples. Under our model configuration with a batch size of

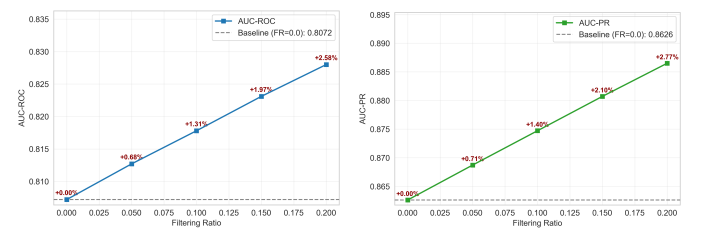


Fig. 3: Performance variation of the distilled model with respect to the passing ratio. The performance consistently improves as the passing ratio increases.

512 and 11 inference iterations for the original uncertainty model, the inference time of the original model is 181.6 ms per iteration, whereas the distilled model achieves 17.9 ms per iteration, reducing it to only 9.86% of the original model.

A key advantage of DAUM is its capacity for indirect passing. Specifically, when focusing on imbalanced metrics, the uncertainty estimated from balanced metrics can be leveraged to pass traffic on the imbalanced ones. We further validate that this indirect passing capability is preserved in the distilled model. We configure different direct passing ratios

and examine the total number of deal samples ultimately passed to downstream tasks, as shown in Figure 4:

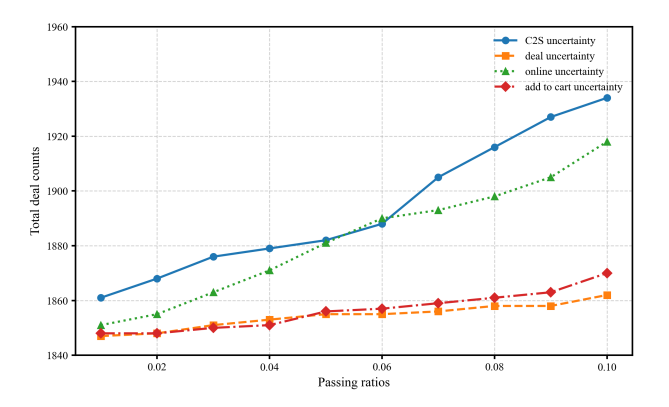
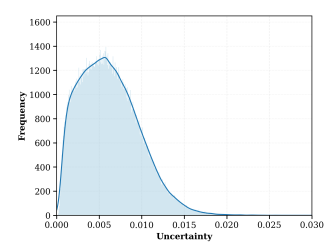


Fig. 4: Total number of deal samples passed to downstream under different passing strategies.

It can be observed that as the passing ratio increases, the uncertainty obtained from C2S click and online remains highly effective in passing the deal metric. Moreover, the overall trend is consistent with that before distillation, indicating that our distilled model remains highly effective, particularly in terms of passing capability.

We further examine the uncertainty distributions of the distilled and original models on the test dataset to assess whether the distilled model has effectively learned the uncertainty information of the original model. The distributions on the training and test datasets are shown in Figure 5.



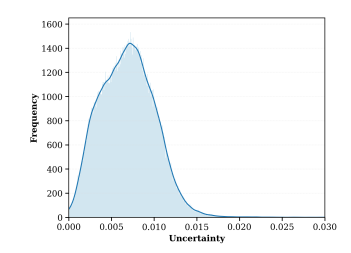


Fig. 5: Uncertainty distributions of the original model (left) and the distilled model (right), with slight differences observed, especially in the high-uncertainty region.

The distilled model preserves the overall distributional pattern on the test dataset, closely matching that of the original uncertainty model. In the high-uncertainty region, which is particularly important for our approach, the two distributions exhibit an even stronger alignment. These observations indicate that the distilled model has successfully retained the underlying behavior of DAUM.

V. CONCLUSION

In this paper, we first provide a mathematical formulation of uncertainty modeling and demonstrate its limitations under label imbalance, where conventional uncertainty estimation becomes unreliable. Building on this analysis, we propose DAUM, which integrates uncertainty modeling with multiobjective learning to overcome these shortcomings and enhance performance in RTA interception scenarios. Furthermore, we develop a lightweight distilled version of DAUM that preserves effective uncertainty estimation while improving inference efficiency by approximately tenfold, thereby enabling the practical deployment of uncertainty modeling in real-time inference. Future research could explore the interrelationships among multiple uncertainties derived from multi-objective learning to further improve estimation quality in sparse-label settings.

REFERENCES

- H. Tang, J. Liu, M. Zhao, and X. Gong, "Progressive layered extraction (ple): A novel multi-task learning (mtl) model for personalized recommendations," in *Proceedings of the 14th ACM conference on recommender systems*, 2020, pp. 269–278.
- [2] J. Ma, Z. Zhao, X. Yi, J. Chen, L. Hong, and E. H. Chi, "Modeling task relationships in multi-task learning with multi-gate mixture-of-experts," in *Proceedings of the 24th ACM SIGKDD international conference on* knowledge discovery & data mining, 2018, pp. 1930–1939.
- [3] X. Ma, L. Zhao, G. Huang, Z. Wang, Z. Hu, X. Zhu, and K. Gai, "Entire space multi-task model: An effective approach for estimating post-click conversion rate," in *The 41st International ACM SIGIR Conference on Research & Development in Information Retrieval*, 2018, pp. 1137– 1140
- [4] C. Blundell, J. Cornebise, K. Kavukcuoglu, and D. Wierstra, "Weight uncertainty in neural network," in *International conference on machine learning*. PMLR, 2015, pp. 1613–1622.
- [5] Y. Gal and Z. Ghahramani, "Dropout as a bayesian approximation: Representing model uncertainty in deep learning," in *international conference on machine learning*. PMLR, 2016, pp. 1050–1059.
- [6] W. J. Maddox, P. Izmailov, T. Garipov, D. P. Vetrov, and A. G. Wilson, "A simple baseline for bayesian uncertainty in deep learning," *Advances in neural information processing systems*, vol. 32, 2019.
- [7] Y. Huang, B. Bai, S. Zhao, K. Bai, and F. Wang, "Uncertainty-aware learning against label noise on imbalanced datasets," in *Proceedings of the AAAI conference on artificial intelligence*, vol. 36, no. 6, 2022, pp. 6960–6969
- [8] M. Sensoy, L. Kaplan, and M. Kandemir, "Evidential deep learning to quantify classification uncertainty," Advances in neural information processing systems, vol. 31, 2018.
- [9] D. Xi, Z. Chen, P. Yan, Y. Zhang, Y. Zhu, F. Zhuang, and Y. Chen, "Modeling the sequential dependence among audience multi-step conversions with multi-task learning in targeted display advertising," in *Proceedings of the 27th ACM SIGKDD Conference on Knowledge Discovery & Data Mining*, 2021, pp. 3745–3755.
- [10] J. Ma, Z. Zhao, J. Chen, A. Li, L. Hong, and E. H. Chi, "Snr: Subnetwork routing for flexible parameter sharing in multi-task learning," in *Proceedings of the AAAI conference on artificial intelligence*, vol. 33, no. 01, 2019, pp. 216–223.
- [11] L. Wang, C. Tang, C. Zhang, J. Ruan, K. Huang, and J. Dai, "Efficient multi-task learning via generalist recommender," in *Proceedings of the* 32nd ACM International Conference on Information and Knowledge Management, 2023, pp. 4335–4339.
- [12] Y. He, X. Feng, C. Cheng, G. Ji, Y. Guo, and J. Caverlee, "Metabalance: improving multi-task recommendations via adapting gradient magnitudes of auxiliary tasks," in *Proceedings of the ACM Web Conference* 2022, 2022, pp. 2205–2215.
- [13] L. Zhang, X. Liu, and H. Guan, "Automtl: A programming framework for automating efficient multi-task learning," Advances in Neural Information Processing Systems, vol. 35, pp. 34216–34228, 2022.
- [14] H. Hazimeh, Z. Zhao, A. Chowdhery, M. Sathiamoorthy, Y. Chen, R. Mazumder, L. Hong, and E. Chi, "Dselect-k: Differentiable selection in the mixture of experts with applications to multi-task learning," Advances in Neural Information Processing Systems, vol. 34, pp. 29335– 29347, 2021.

- [15] J. Zhou, X. Cao, W. Li, L. Bo, K. Zhang, C. Luo, and Q. Yu, "Hinet: Novel multi-scenario & multi-task learning with hierarchical information extraction," in 2023 IEEE 39th International Conference on Data Engineering (ICDE). IEEE, 2023, pp. 2969–2975.
- [16] A. Kendall, Y. Gal, and R. Cipolla, "Multi-task learning using uncertainty to weigh losses for scene geometry and semantics," in *Proceedings of the IEEE/CVF Conference on Computer Vision and Pattern Recognition (CVPR)*, 2018, pp. 7482–7491.
- [17] Z. Xu, P. Wei, W. Zhang, S. Liu, L. Wang, and B. Zheng, "Ukd: Debiasing conversion rate estimation via uncertainty-regularized knowledge distillation," in *Proceedings of the ACM Web Conference* 2022, 2022, pp. 2078–2087.
 [18] I. Achituve, A. Navon, G. Chechik, and T. Raviv, "Bayesian uncertainty
- [18] I. Achituve, A. Navon, G. Chechik, and T. Raviv, "Bayesian uncertainty for gradient aggregation in multi-task learning," in *International Con*ference on Learning Representations (ICLR), 2024.
- [19] H. Wang, Z. Sun, Y. Du, L. Zhang, T. He, and Y.-S. Ong, "Uncertain multi-objective recommendation via orthogonal meta-learning enhanced bayesian optimization," *arXiv* preprint *arXiv*:2502.13180, 2025.